Double-resonance response of a superconducting quantum metamaterial: Manifestation of nonclassical states of photons

M. A. Iontsev,[1] S. I. Mukhin,[1] and M. V. Fistul[1,2,3]
[1]*Theoretical Physics and Quantum Technologies Department, National University of Science and Technology "MISIS", 119049 Moscow, Russia*
[2]*Theoretische Physik III, Ruhr-Universität Bochum, D-44801 Bochum, Germany*
[3]*Russian Quantum Center, 143025 Moscow Region, Russia*
(Received 6 July 2016; revised manuscript received 26 September 2016; published 17 November 2016)

We report a theoretical study of the ac response of superconducting quantum metamaterials (SQMs), i.e., an array of qubits (two-level systems) embedded in a low-dissipative resonator. By making use of a particular example of a SQM, namely the array of charge qubits capacitively coupled to the resonator, we obtain a second-order phase transition between an incoherent (the high-temperature phase) and coherent (the low-temperatures phase) state of photons. This phase transition in many aspects resembles the paramagnetic-ferromagnetic phase transition. The critical temperature of the phase transition, $T^{\star}$, is determined by the energy splitting of two-level systems δ, number of qubits in the array N, and the strength of the interaction η between qubits and photons in the cavity. We obtain that the photon states manifest themselves by resonant drops in the frequency-dependent transmission $D(\omega)$ of electromagnetic waves propagating through a transmission line weakly coupled to the SQM. At high temperatures the $D(\omega)$ displays a single resonant drop, and at low temperatures a peculiar double-resonance response has to be observed. The physical origin of such a resonant splitting is the quantum oscillations between two coherent states of photons of different polarizations.

DOI: 10.1103/PhysRevB.94.174510

I. INTRODUCTION

Great attention is devoted to a theoretical and experimental study of novel superconducting quantum metamaterials (SQMs) [1–10]. The SQMs consist of an array of superconducting qubits, e.g., charge qubits [11], flux qubits [12], and transmons [13], embedded in a low-dissipative resonator. Various macroscopic quantum coherent effects, such as coherent quantum oscillations between two states, microwave-induced Rabi oscillations, and Ramsey fringes, just to name a few, have been observed in the SQMs. Moreover, since a strong long-range interaction between qubits is provided by exchange of resonators photons, one can expect a strong variation of the energy spectrum of the SQMs with respect to a set of noninteracting qubits and, therefore, various collective coherent quantum effects in the SQMs. Indeed, in the Ref. [6] instead of a large amount of small different splittings, a single giant splitting has been observed in the spectrum of the SQM, and this effect indicates the presence of collective quantum beatings in the SQM.

The various quantum mechanical phenomena manifest themselves by resonant drops in the frequency-dependent transmission coefficient $D(\omega)$ of electromagnetic waves propagating through the transmission line coupled (inductively or capacitively) to the SQM [3–6]. Such measurement setup is presented schematically in Fig. 1. The theoretical analysis allowing one to express the transmission coefficient $D(\omega)$ in terms of the quantum-mechanical time-dependent correlation function of a system of qubits has been done in Ref. [14].

On the other hand, the interaction of photons with an array of qubits results not only in the change of qubits spectrum but also it can lead to the appearance of novel photon states in the SQMs [8–10,15,16]. For example, it was predicted for the chain of small Josephson junctions [15] and later for the chain of SQUIDS biased in the macroscopic quantum regime, i.e., flux qubits [16], that at low temperatures the coherent state of photons occurs. Moreover, the second-order phase transition between the incoherent state of photons (the high-temperature phase) and the coherent state of photons (the low-temperature phase) has been established [16]. However, the physical properties of the low-temperature phase have not been studied yet, and the analysis of the transmission coefficient $D(\omega)$ for different photonic states has not been carried out.

Therefore, in this article by making use of a specific SQM, i.e., an array of charge qubits capacitively coupled to the resonator (see Fig. 1), we provide an analysis of both the phase transition and physical properties of the photon states in the low-temperature phase. By making use of a generic study of the transmission coefficient $D(\omega)$ we show that in the high-temperature phase of photons the $D(\omega)$ shows a single resonant drop at the photon frequency ω_{ph}. In contrast, the low-temperature phase of photons manifests itself by a single drop at low frequency ω_R and a peculiar double-resonance response at frequencies, $\omega_{ph} \pm \omega_R$. This phenomena has an origin in the quantum beating between the coherent states of photons of different polarizations, and ω_R is the frequency of such beatings.

The paper is organized as follows: In Sec. II we present a particular model and elaborate the Hamiltonian and the effective action of the SQM. In Sec. III we analyze in detail the phase transition in the photonic states. Especially, we will discuss the properties of the coherent low-temperature phase. In Sec. IV we apply the generic analysis in order to obtain the transmission coefficient $D(\omega)$ for different photonic states in the SQMs. Section V provides conclusions.

II. MODEL, HAMILTONIAN, AND EFFECTIVE ACTION OF SQM

Let us to consider a particular SQM containing the array of N small voltage gated Josephson junctions, i.e., charge qubits. Each qubit is capacitively coupled to the resonator. The

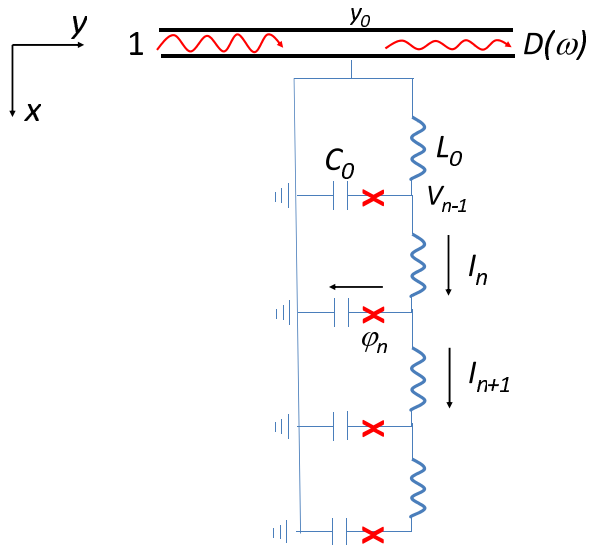

FIG. 1. The schematic of the measurements setup: the transmission line inductively coupled to the particular SQM, i.e., an array of charge qubits embedded in the resonator.

schematic of such SQM is presented in Fig. 1. The classical description of the SQM is based on the Lagrangian formalism, and the Lagrangian of the whole system, i.e., the array of qubits interacting with the resonator, consists of three parts: the photons field, the array of Josephson junctions, and the interaction between them:

$$L = L_{ph} + L_{JJ} + L_{int}. \tag{1}$$

The explicit expression for the Lagrangian is derived from the classical equation of motion, where the resonator is characterized by time-dependent current and voltage distributions, I_n and V_n, and the dynamics of a single Josephson junction is described by the time-dependent Josephson phase, $\varphi_i(t)$. These equations are written as

$$I_{n+1} - I_n = I_c \sin(\varphi_n) + \frac{\hbar C_J}{2e}\frac{d^2\varphi_n}{dt^2} = C_0\frac{d}{dt}\left[V_n - \frac{\hbar}{2e}\frac{d\varphi_n}{dt}\right],$$
$$V_n - V_{n-1} = L_0\frac{dI_n}{dt}, \tag{2}$$

where C_0 and L_0 are the capacitance and the inductance per unit length of the resonator; I_c and C_J are the critical current and the capacitance of a Josephson junction, accordingly. In the continuum limit we introduce the coordinate-dependent charge distribution, $Q(x,t)$, as $I(x,t) = dQ(x,t)/dt$ (x is the coordinate along the resonator). By making use of the analysis elaborated in [16–18] we obtain

$$L_{ph} = m\left[\dot{Q}^2 - c_0^2\left(\frac{\partial Q}{\partial x}\right)^2\right], \tag{3}$$

where the effective mass $m = L_0 l/2$; l is the length of the resonator, and c_0 is the velocity of electromagnetic waves in the resonator.

The Lagrangian of the array of N small Josephson junctions L_{JJ} is written as

$$L_{JJ} = E_J\sum_i\left\{\frac{1}{2\omega_p^2}\left[\dot{\varphi}_i + \sqrt{\frac{C_0}{C_J}}2eV_i/\hbar\right]^2 - [1-\cos\varphi_i]\right\}, \tag{4}$$

where E_J is the Josephson coupling energy, and ω_p is the plasma frequency of the Josephson junction.

The last part of Lagrangian describes the capacitive interaction between the electromagnetic field and the array of Josephson junctions:

$$L_{int} = \frac{\hbar}{2e}\sum_i Q(t,x_i)\dot{\varphi}_i. \tag{5}$$

Next, we greatly simplify a whole problem by taking into account the interaction of arrays of qubits with a *single cavity mode*. This assumption is valid for a low-dissipative resonator in the frequency range of $\omega \leqslant \omega_{ph}$ as all self-frequencies of the resonator are well separated from each other. In this case the photon mode $Q(x,t) = Q(t)\cos(k_n x)$, where k_n are the wave vectors of cavity modes. Substituting this expression in Eqs. (3) and (5) we obtain

$$L_{ph} = \frac{m}{2}\left(\dot{Q}^2 - \omega_0^2 Q^2\right), \tag{6}$$

where $\omega_0 = c_0 k_n$ is the photon frequency of the resonator. The interacting Lagrangian is written in the following form:

$$L_{int} = \sum_i \tilde{\eta}_i Q(t)\dot{\varphi}_i, \tag{7}$$

where $\tilde{\eta}_i = \frac{\hbar}{2e}\cos(k_n x_i)$. With an assumption that the size of the array of qubits is much smaller than the resonator size, all parameters $\tilde{\eta}_i$ are equal to $\tilde{\eta}$.

The equilibrium state of the SQM is described by the partition function Z that can be written through the path integral in the imaginary-time representation as

$$Z = \int D[Q]D[\varphi_i]\exp\left\{-\frac{1}{\hbar}\int_0^{\hbar/k_BT} d\tau L[Q(\tau),\varphi_i(\tau)]\right\}. \tag{8}$$

In order to describe the quantum dynamics of small Josephson junctions array interacting with the resonator electromagnetic field, we consider the particular case as all V_i are equal to the same value of $eV_0 = \sqrt{C_J/C_0}(\hbar\omega_p)^2/4E_J$. In this case the quantum dynamics of a single Josephson junction is truncated to the dynamics of a two-level system (TLS) [11]; i.e., the Hamiltonian H_{JJ} of Josephson junctions array is written as

$$H_{TLS} = \delta\sum_i \sigma_x^{(i)}, \tag{9}$$

where 2δ is the splitting between energy levels of the TLS. In the particular case of the array of charge qubits, $2\delta = E_J$. Correspondingly, the interaction of TLSs with the electromagnetic field of the resonator is described by the Hamiltonian, H_{int}, as

$$\hat{H}_{int} = \eta Q(t)\sum_i \hat{\sigma}_z^{(i)}, \tag{10}$$

where $\eta = \frac{\hbar^2\omega_p^2}{2E_J}\tilde{\eta}/\hbar$, and $\hat{\sigma}_z$, $\hat{\sigma}_x$ are the corresponding Pauli matrices. In adiabatic regime as the self-frequency of the resonator ω_0 is less than $\delta/\hbar$ we obtain the adiabatic energy levels: $E_\pm = \pm\sqrt{\delta^2 + (\eta Q)^2}$ of a single qubit interacting with the electromagnetic field of the resonator. For such adiabatic levels the partition function of an array of qubits interacting with electromagnetic field is $Z_{\text{qubits}} = \prod_{i=1}^{N} \cosh[E_+/(2k_BT)]$. By making use of the procedure elaborated in Ref. [16] we trace the expression of the partition function Z [Eq. (8)] over the variables φ_i and obtain the effective nonlinear Lagrangian which depends on the photon variable Q only:

$$Z_{\text{eff}} = \int D[Q] \exp\left\{-\frac{1}{\hbar}\int_0^{\hbar/k_BT} d\tau L_{\text{eff}}[Q(\tau)]\right\},$$
$$L_{\text{eff}} = \frac{m}{2}\left[\dot{Q}^2 + \omega_0^2 Q^2\right] - k_BTN \ln\cosh\left[\frac{\sqrt{\delta^2 + (\eta Q)^2}}{2k_BT}\right]. \quad (11)$$

Thus, one can see that the interaction of photons of resonators with the array of qubits results in the effective nonlinear interaction between photons.

III. PHASE TRANSITION IN STATES OF PHOTONS

The photonic states stabilized in the SQMs are essentially determined by the type of the effective Q-dependent potential

$$U(Q) = \frac{m}{2}\omega_0^2 Q^2 - k_BTN \ln\cosh\left[\frac{\sqrt{\delta^2 + (\eta Q)^2}}{2k_BT}\right]. \quad (12)$$

The potential changes its form at the transition temperature $T^\star = \delta\{k_B \ln[(1+\alpha)/(1-\alpha)]\}^{-1}$, where the parameter $\alpha = \frac{2m\delta\omega_0^2}{N\eta^2}$. At high temperatures, i.e., $T > T^\star$, the $U(Q)$ has a single minimum at $Q = 0$ [see Fig. 2(a), blue line]. In this case the photon state is the *incoherent one*, and the thermal distribution of photons over the Fock states occurs [19]. The interaction between photons results in a decrease of the frequency of photons, ω_{ph}, to $\omega_1 = \omega_0\sqrt{1 - \frac{1}{\alpha}\tanh\frac{\delta}{2k_BT}}$. For the incoherent state of photons the Kerr type of nonlinearity, $KQ^4/4$, occurs in the SQM. The Kerr constant K has a following form:

$$K(T) = \frac{N}{\eta^4}4\delta^3\left[\tanh(x) - \frac{x}{\cosh^2(x)}\right], x = \delta/(2k_BT). \quad (13)$$

The Kerr constant is rather small in the limit $T \gg T^\star$. The temperature dependence of K is shown in Fig. 2(b).

However, at low temperatures $T \leqslant T^\star$ the effective potential $U(Q)$ has two minima at $Q_\pm$ separated by the maximum at $Q = 0$ [see Fig. 2(a), red line]. At temperatures that are not far from the transition temperature $T^\star$ the values $Q_\pm$ are still small, and it is written explicitly as $Q_\pm = \pm\sqrt{\frac{m|\omega_1|^2}{K}}$. Each minimum corresponds to the *coherent state* of photons [19]. These states are characterized by nonzero values of the quantum-mechanical average of the charge amplitude, $\langle Q\rangle = Q_\pm$, and the Poissonian distribution of photons over

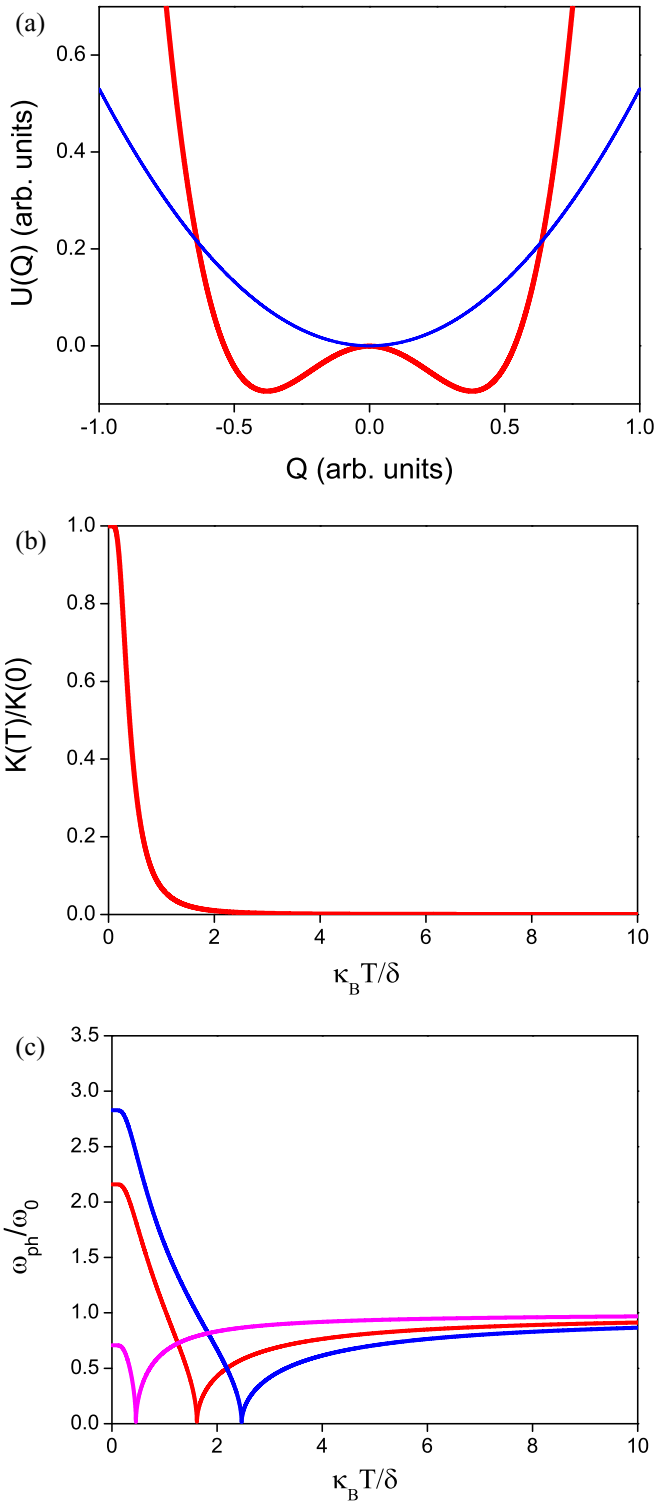

FIG. 2. (a) The effective potential $U(Q)$ describing the interaction of photons in the SQM: high-temperature incoherent phase (blue line, $k_BT = 3.3\delta$) and low-temperature coherent phase (red line, $k_BT = 0.7\delta$). (b) The temperature dependence of the Kerr nonlinearity parameter $K(T)$. For panels (a) and (b) the value of parameter $\alpha = 0.3$ was used. (c) The temperature dependence of the photon frequency ω_{ph}, i.e., ω_1 for $T > T^\star$ and ω_2 for $T < T^\star$, for different parameters $\alpha = 0.2$ (blue line), $\alpha = 0.3$ (red line), and $\alpha = 0.8$ (magenta line).

the Fock states [19]. The frequency of such photon field is also renormalized, to $\omega_2 = \omega_0\sqrt{2(\frac{1}{\alpha}\tanh\frac{\delta}{2k_BT} - 1)}$. The temperature dependence of the photon frequency in a whole range of temperature is shown in Fig. 2(c) for different values of parameter α.

Moreover, these two coherent states of photons are degenerate states having the same energy but they differ by the polarization of electromagnetic field. These two polarizations are characterized by the phase of the electromagnetic field, ϕ, which can take two definite values, 0 and π. Both states correspond to a well-known "lasing" electromagnetic field [19]. However, close to the transition temperature as the $Q_\pm$ is small, the macroscopic quantum tunneling through the barrier [see Fig. 2(a)] results in a small splitting Δ between these two coherent photonic states. As a consequence the coherent quantum Rabi oscillations between these macroscopic quantum photon states with the frequency $\omega_R = \Delta/\hbar$ can be established. The frequency of such oscillations is small, and it is obtained in the quasiclassical approximation as

$$\omega_R = \Delta/\hbar = \omega_2 \exp\left[-\frac{2}{3\hbar}\sqrt{2mK(T)}Q_+^3\right]. \quad (14)$$

Notice here that in the limit $T \to 0$ and for a large number of qubits N, the number of photons in the coherent state that is proportional to $Q_\pm$ is also large, and the tunneling exponent becomes exponentially small: $\sim \exp -N^2$. Hence, the tunneling vanishes and the photonic condensate breaks the symmetry by choosing phase of the electromagnetic wave either 0 or π. Therefore, our analysis provides a direct possibility of visualizing the transition from quantum few-phonon coherent states with Rabi oscillations and characteristic frequency ω_R, to the classical "lasing" electromagnetic field.

IV. AC RESPONSE OF A QUANTUM METAMATERIAL

As was shown in Ref. [14] the coherent quantum-mechanical oscillations arising in the SQM are directly observed by measurements of electromagnetic wave (EW) propagation in the transmission line coupled to the SQM. Similarly, the different states of photons considered in the Sec. III manifest themselves in the frequency-dependent transmission coefficient, $D(\omega)$. The measurement setup allowing such observation is shown in Fig. 1. The EW propagation in the transmission line is determined by the following equation:

$$\frac{1}{c_0^2}\frac{\partial^2 q(y,t)}{\partial t^2} - \frac{\partial^2 q}{\partial y^2} = \kappa\delta(y - y_0)Q(y_0,t), \quad (15)$$

where y is the coordinate along the transmission line, $q(y,t)$ is the charge distribution in the EW, and κ is the inductive coupling between the transmission line and the SQM. The Hamiltonian of the SQM interacting with the EWs in the transmission line is written as

$$\hat{H} = \hat{H}_{SQM} - \kappa q(y_0,t)Q(y_0,t). \quad (16)$$

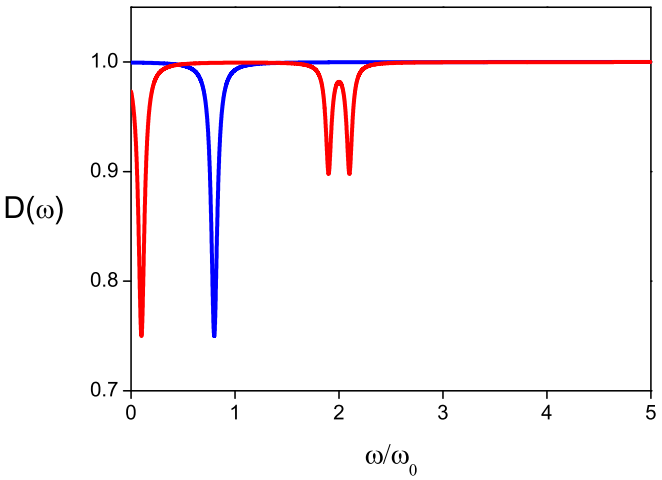

FIG. 3. The frequency-dependent transmission coefficient $D(\omega)$ for the incoherent (blue curve) and coherent (red curve) photon states. The parameters $\omega_1 = 0.8\omega_0$ corresponding to the temperature $k_BT = 4\delta$, $\omega_2 = 2\omega_0$ ($k_BT = \delta$), $\omega_R = 0.1\omega_0$, and $\gamma = 0.03\omega_0$ were used.

The right-hand part of Eq. (15) is determined by the quantum-mechanical average of $Q(t)$, i.e.,

$$\langle Q(t)\rangle = \kappa\int_0^t ds\,\chi_{QQ}(t-s)q(s),$$

where $\chi_{QQ}(t) = \frac{i}{\hbar}\langle[Q(t),Q(0)]\rangle$ is the imaginary part of the correlation function $C(t)$ [20]. By making use of the Fourier transformation we arrive at the well-known problem of the propagation of EWs in the 1D channel in the presence of a single scatterer. Thus, we obtain the transmission coefficient as

$$D(\omega) = \frac{1}{1 + \frac{c\kappa\,\mathrm{Im}(\chi_{QQ})}{\omega}}. \quad (17)$$

Therefore, the singularities of the $\chi_{QQ}(\omega)$ determine the resonant drops in the $D(\omega)$ dependence. In the high-temperature incoherent photon state the $\chi_{QQ}(\omega)$ is the response function of the harmonic oscillator of the frequency ω_1. By making use of a standard analysis [20] we obtain

$$\chi_{QQ}^{\mathrm{incoh}}(\omega) = \frac{1}{2m\omega_1}\frac{1}{\omega_1 - \omega - i\gamma}, \quad (18)$$

where γ is the dissipation parameter. Therefore, the frequency dependence $D(\omega)$ shows a single resonant drop at the frequency ω_1 (see Fig. 3, blue curve) as the incoherent state of photons occurs in the SQM.

The situation drastically changes for the low-temperature phase, where the photonic states have four low-lying coherent states with the energies $E_{1,2} = \pm\Delta/2$, $E_{3,4} = \hbar\omega_2 \pm \Delta/2$. Moreover, the external EW can excite the transitions between different parity states, i.e., $E_1 \to E_2$, $E_1 \to E_4$, and $E_2 \to E_3$. By making use of the generic expression [20]

$$C(t) = \sum_n \rho_n \sum_m \exp[i(E_n - E_m)t]|\langle m|Q|n\rangle|^2, \quad (19)$$

where ρ_n is the equilibrium density matrix and $\langle m|Q|n\rangle$ are the matrix elements for the Q operator, the quantum-mechanical

correlation function of the low-temperature photonic state contains three resonant terms:

$$\chi^{\rm coh}(\omega) = \frac{Q_+^2}{\omega_R - \omega - i\gamma} + \frac{\hbar}{m\omega(\omega_2 + \omega_R - \omega - i\gamma)} + \frac{\hbar}{m\omega(\omega_2 - \omega_R - \omega - i\gamma)}. \quad (20)$$

It leads to a single drop at low frequencies $\simeq\omega_R$ and a double-resonant drop around the photon frequency ω_2 in the frequency dependence of the transmission coefficient $D(\omega)$ (see Fig. 3, red line). Therefore, such resonant structure of the frequency-dependent transmission coefficient is a fingerprint of macroscopic quantum oscillations between two coherent states of photons.

V. DISCUSSION AND CONCLUSIONS

The observation of predicted effects can be made in the setup schematically shown in Fig. 1. The experimental realization of such setup is an array of qubits incorporated in a coplanar waveguide [4–6]. The typical values of energy level difference $\delta/h \simeq 5$ GHz, and the photon frequency $\omega_0 \simeq$ 500 MHz has to be chosen to establish the adiabatic regime. The length of resonator $\ell = \lambda/2$, where λ is the wave length, allows us to incorporate in the resonator up to 1000 qubits. The transition temperature $T^\star$ is mostly determined by the ratio of two capacitances, C_0 and C_J ($C_0 \ll C_J$), and therefore, $T^\star$ is tunable in a wide region: from $T^\star \simeq 100\delta/k_B \simeq$ 25 K ($\alpha = 0.02$) to $\simeq 0.5\delta/k_B \simeq 125$ mK ($\alpha \simeq 0.7$). Moreover, the double-resonance frequency splitting $\omega_R \simeq$ 10–100 MHz can be observed for temperatures close to the transition temperature. A crucial condition to observe the phase transition in photon states and quantum beatings between two coherent states of photons is a low dissipation in the SQM, i.e., $\gamma < \omega_R$. Notice here that these effects are not washed out in the presence of a weak disorder in qubits and resonator parameters, i.e., δ, η, and α. However, a slight detuning of qubits from the symmetry point results in the additional term proportional to $\hat{\sigma}_z$ in the Hamiltonian [Eq. (9)], and in this case the symmetry between two coherent photon states is broken, and the double-resonant response cannot be observed.

In conclusion we have studied the various equilibrium photon states occurring in the SQM, i.e., an array of superconducting qubits embedded in a low-dissipative resonator. We considered the adiabatic nonresonant regime as the photon energy of resonator $\hbar\omega_0$ is much smaller than the energy splitting of qubits, δ. In this regime we obtained the second-order phase transition in the states of photons. At high temperatures $T > T^\star$ the incoherent state of photons can be realized. In this case the interaction between photons and qubits results in a substantial decrease of the photon frequency as the temperature becomes closer to the transition temperature $T^\star$ [see Fig. 2(c)]. Moreover, the temperature-dependent Kerr type of nonlinearity having a quantum origin occurs in the SQM [see Fig. 2(b)]. At low temperatures ($T < T^\star$) the coherent states of photons with two different polarizations occur in such a SQM. The frequency of coherent photons increases with temperature [see Fig. 2(c)]. The density of photons in these states is determined by the macroscopic value of $Q_\pm$. Each state corresponds to a well-known "lasing" electromagnetic field. However, it is most interesting that these two macroscopic coherent states of photons have equal energies, but they are divided by the barrier. Thus, the coherent quantum oscillations of frequency ω_R between coherent states of photons can be provided by quantum tunneling through the barrier [see Fig. 2(a)]. The frequency ω_R is determined by Eq. (14).

By making use of an analysis of the EW propagation in the transmission line coupled to the SQM (see setup in Fig. 1) we obtain that different photon states manifest themselves as resonant drops in the frequency-dependent transmission coefficient $D(\omega)$ (see Fig. 3). The incoherent state of photons displays a single drop at $\omega = \omega_1$ but the coherent state of photons has to show three resonant drops: at small frequency ω_R and double-resonant drop at frequencies $\omega_2 \pm \omega_R$. The observation of such resonant structure in the $D(\omega)$ dependence provides direct evidence of macroscopic quantum oscillations between two coherent states of photons.

ACKNOWLEDGMENTS

We acknowledge financial support from the Ministry of Education and Science of the Russian Federation in the frame of the Increase Competitiveness Program of the NUST MISIS (Contract No. K2-2014-015). M.V.F. acknowledges hospitality of the International Institute of Physics, Natal, Brazil, where this work was finished.

[1] A. M. Zagoskin, *Quantum Engineering: Theory and Design of Quantum Coherent Structures* (Cambridge University Press, Cambridge, 2011), pp. 272-311; A. L. Rakhmanov, A. M. Zagoskin, S. Savel'ev, and F. Nori, Phys. Rev. B **77**, 144507 (2008).

[2] P. Jung, A. V. Ustinov, and S. M. Anlage, Supercond. Sci. Technol. **27**, 073001 (2014).

[3] Z.-L. Xiang, S. Ashhab, J. Q. You, and F. Nori, Rev. Mod. Phys. **85**, 623 (2013).

[4] J. M. Fink, R. Bianchetti, M. Baur, M. Göppl, L. Steffen, S. Filipp, P. J. Leek, A. Blais, and A. Wallraff, Phys. Rev. Lett. **103**, 083601 (2009).

[5] M. Jerger, S. Poletto, P. Macha, U. Huebner, A. Lukashenko, E. Il'ichev, and A. V. Ustinov, Europhys. Lett. **96**, 40012 (2011).

[6] P. Macha, G. Oelsner, J.-M. Reiner, M. Marthaler, S. Andre, G. Schön, U. Huebner, H.-G. Meyer, E. Il'ichev, and A. V. Ustinov, Nat. Commun. **5**, 5146 (2014).

[7] D. S. Shapiro, P. Macha, A. N. Rubtsov, and A. V. Ustinov, Photonics **2**, 449 (2015).

[8] M. Koppenhöfer, M. Marthaler, and G. Schön, Phys. Rev. A **93**, 063808 (2016).
[9] H. Asai, S. Savel'ev, S. Kawabata, and A. M. Zagoskin, Phys. Rev. B **91**, 134513 (2015); H. Asai, S. Kawabata, A. M. Zagoskin, and S. E. Savel'ev, arXiv:1605.04929.
[10] Z. Ivic, N. Lazarides, and G. P. Tsironis, Sci. Rep. **6**, 29374 (2016).
[11] Y. Nakamura, Yu. A. Pashkin, and J. S. Tsai, Nature (London) **398**, 786 (1999).
[12] I. Chiorescu, Y. Nakamura, C. J. P. M. Harmans, and J. E. Mooij, Science **299**, 1869 (2003).
[13] J. Koch, T. M. Yu, J. Gambetta, A. A. Houck, D. I. Schuster, J. Majer, A. Blais, M. H. Devoret, S. M. Girvin, and R. J. Schoelkopf, Phys. Rev. A **76**, 042319 (2007).
[14] P. A. Volkov and M. V. Fistul, Phys. Rev. B **89**, 054507 (2014).
[15] J. K. Harbaugh and D. Stroud, Phys. Rev. B **61**, 14765 (2000).
[16] S. I. Mukhin and M. V. Fistul, Supercond. Sci. Technol. **26**, 084003 (2013).
[17] M. Wallquist, J. Lantz, V. S. Shumeiko, and G. Wendin, New J. Phys. **7**, 178 (2005).
[18] A. Blais, R.-S. Huang, A. Wallraff, S. M. Girvin, and R. J. Schoelkopf, Phys. Rev. A **69**, 062320 (2004).
[19] R. Loudon, *The Quantum Theory of Light* (Oxford University Press, New York, 1973).
[20] G.-L. Ingold, Lect. Notes Phys. **611**, 1 (2002).